Stochastic representation for anisotropic permeability tensor random fields

Johann Guilleminot, Christian Soize, R. Ghanem

Stochastic representation for anisotropic permeability tensor random fields*

J. Guilleminot[1], C. Soize[1] and R. G. Ghanem[2]

[1]Université Paris-Est
Laboratoire MSME UMR8208 CNRS
5 Bd Descartes, 77454 Marne la Vallée, France

[2]University of Southern California
210 KAP Hall, Los Angeles, CA 90089, USA

Published online: 6 SEP 2011

Abstract

In this paper, we introduce a novel stochastic model for the permeability tensor associated with stationary random porous media. In the light of recent works on mesoscale modeling of permeability, we first discuss the physical interpretation of the permeability tensor randomness. Subsequently, we propose a non-parametric prior probabilistic model for non-Gaussian permeability tensor random fields, making use of the information theory and a MaxEnt procedure, and provide a physical interpretation of the model parameters. Finally, we demonstrate the capability of the considered class of random fields to generate higher levels of statistical fluctuations for selected stochastic principal permeabilities. This unique flexibility offered by the parameterisation of the model opens up many new possibilities for both forward simulations (e.g. for uncertainty propagation in predictive simulations) and stochastic inverse problem solving.

Keywords: Transport properties; Random Media; Probabilistic methods; Random field; Permeability tensor.

Notations

Let $\mathbb{M}_d^S(\mathbb{R})$ and $\mathbb{M}_d^+(\mathbb{R}) \subset \mathbb{M}_d^S(\mathbb{R})$ be the sets of all the $(d \times d)$ real symmetric matrices and $(d \times d)$ real symmetric positive-definite matrices, respectively. Let $[I_d]$ be $(d \times d)$ identity matrix. Let $\det([A])$ and $[A]^{\mathrm{T}}$ be the determinant and transpose of matrix $[A]$, respectively.

For any real symmetric matrices $[A]$ and $[B]$, inequality $[A] > [B]$ denotes Loewner (partial) ordering, that is to say, $[A] > [B]$ means that the matrix $[A] - [B]$ is positive-definite.

*J. Guilleminot, C. Soize and R. Ghanem, Stochastic representation for anisotropic permeability tensor random fields, International Journal for Numerical and Analytical Methods in Geomechanics, 36(13), 1592-1608, DOI: 10.1002/nag.1081 (2012).

Let $\|\cdot\|_{\mathrm{F}}$ be the Frobenius (or Hilbert-Schmidt) norm, defined as $\|[A]\|_{\mathrm{F}}^2 = \mathrm{Tr}\left([A]^2\right)$ for any real symmetric matrix $[A]$. Let $\mathbf{x}$ and $\mathbf{y}$ be two real vectors in $\mathbb{R}^p$. We denote by $\mathbf{x}\cdot\mathbf{y}$ the Euclidean inner product, $\mathbf{x}\cdot\mathbf{y} = \sum_{i=1}^{p} \mathbf{x}_i \mathbf{y}_i$.

Finally, let E be the mathematical expectation.

1 Introduction

The study of fluid flows through porous media is an important field of both research and engineering, which has received a large attention from the scientific community during the past decades. Such an issue arises in various fields of applications, such as hydrogeology, petroleum engineering or composite manufacturing (in liquid composite molding (LCM) processes). Hereafter, we consider the case of stationary flows (at low Reynolds number) which can be described, at the scale under consideration, by Darcy's law:

$$\mathbf{v} = -\frac{1}{\mu}[K]\boldsymbol{\nabla} p, \tag{1}$$

wherein $\mathbf{v} \in \mathbb{R}^d$ and $\boldsymbol{\nabla} p \in \mathbb{R}^d$ are the (volume averaged) flow velocity and pressure gradient respectively; μ is the fluid viscosity and $[K]$ is the symmetric positive-definite matrix representation, in the canonical basis of $\mathbb{R}^d$, of the second-order (intrinsic) *permeability* tensor of the porous medium (the term *hydraulic conductivity* being also widely used in Earth sciences). Note that the acceleration due to gravity is neglected but can easily be accounted for in equation (1).

No matter the field of application, it is well recognized that the modeling of the permeability tensor field is of primal importance for predictive simulations to be obtained, since it controls both the direction and magnitude of the flow. Such an issue is, in fact, all the more critical that the inverse identification is often an ill-posed problem [1], so that the derivation of a relevant *prior* algebraic stochastic model, synthesizing as many information as possible (such that the anisotropy of the tensor, etc.) and depending on a limited number of parameters (allowing for an inverse identification with limited experimental data), is highly desirable. In this study, we consider the case where the permeability tensor randomly and significantly fluctuates from point of the domain to another. Such a situation typically arises while modeling soil heterogeneity (see the recent synthesis by Rubin [2]). This paper is therefore devoted to the construction of a prior stochastic representation for non-Gaussian anisotropic permeability tensor random fields. One may note at this stage that as soon as the proposed model has been calibrated from experimental measurements (by solving a stochastic inverse problem), it can be readily used for uncertainty propagation (UP) and for assessing, having recourse to a probabilistic convergence analysis, the size of the Representative Volume Element (RVE) associated with darcean flow through the considered random porous medium, for instance. For the sake of brevity, we do not specifically address this technical aspect and refer the interested reader to the very large literature available on the subject; see [3] [4] [5] for reviews and applications in fluid mechanics for instance, as well as the general survey proposed in [6].

The paper is organized as follows. We first discuss, in Section 2, the nature of the randomness which is usually exhibited by permeability tensors. In particular, we introduce the fundamental notion of scale separation and the resulting concept of random uncertainties arising at the mesoscale. Two key properties, which have important consequences regarding the methodology followed for deriving the model, are further recalled. We subsequently propose, in Section 3, a complete probabilistic framework and a prior stochastic model for non-Gaussian permeability tensor random fields, the construction of which is performed within the framework of information theory and having recourse to the Maximum Entropy approach. In Section 4, we finally provide an application which takes advantage of the parameterisation of the non-parametric

formulation. It will be shown that unlike the other non-parametric model derived in the literature [7], the proposed approach allows for the propagation of higher uncertainties in given directions and therefore, turns out to be especially suitable for forward simulations of Darcean flows and inverse problem solving.

2 Multiscale framework for stochastic modeling of permeability tensors

In many practical applications involving Darcean flows, the porous medium may be considered as a random media, that is to say, the characteristic functions describing the microstructure of the material are random fields. In particular, the porosity and connectivity of the pore space, which are both known to have a significant influence on the flow (see [8] [9] for instance) do significantly and randomly fluctuate from one point of the domain to another. In the following, we consider the case of a steady single-phase fluid flow through a porous medium which is assumed to be stationary, that is to say, all the systems of marginal probability distributions of the random fields (indexed by $\mathbb{R}^{d^*}$, $1 \leq d^* \leq 3$) describing the local microstructure are invariant under translation in $\mathbb{R}^{d^*}$. In this context, it is well known that Darcy's law is the effective constitutive equation resulting from the homogenization of the Stokes equation governing the fluid behaviour at the microscale; see [10] among many others. Consequently, there are some straightforward analogies between the resulting formulation and the one derived in stochastic homogenization for heterogeneous materials, as well as between the features exhibited by permeability and overall (homogenized) elasticity tensors. One may note, however, that there is no constitutive equation governing the flow at microscale, and that the permeability is intrinsically scale-dependant (while elastic properties are not; see the discussion in [9]). In particular, depending on some morphological properties of the pore space (e.g. the characteristic size of the pores), the so-called *scale separation* may not exist. In other words, the size of RVE for the Darcean flow may not be sufficiently "small" in comparison to the characteristic length of the macroscale, for which the remaining statistical fluctuations (induced by the random microstructure of the medium) can not be neglected anymore and have to be taken into account within a probabilistic framework. This key concept of scale separation is illustrated in Figure 1, where a flow front (moving from the left to the right side) is schematically represented at times t and $t + \Delta t$, together with the RVE size associated with the random medium. In such situations, the domain used for a computational analysis (resulting from the spatial/time discretization) or in experimental testing is likely to be (much) smaller than the RVE and consequently, the permeability tensor has to be modeled as a random field, which will require the use of some advanced stochastic representations that will be introduced later. Such an issue is of primal importance in geomechanics, in which typical applications may involve random microstructures for which the RVE (for Darcean flows) may be several square-meters in cross-section.

Before addressing the modeling further, it is very instructive to characterize some specific properties exhibited by the permeability at such a scale, which is usually referred to as a *mesoscale*. For the sake of simplicity, let us fix the spatial location at point, say $\mathbf{x}_0$, of the medium and consider an open bounded domain Ω in $\mathbb{R}^d$, centered on $\mathbf{x}_0$ and corresponding to a mesoscopic volume. Let $\partial\Omega$ be the boundary of Ω. The properties of the apparent permeability tensor have been studied by numerous authors in the context of saturated flows [11] [12]; see also [13] for a numerical characterization of size effects. A thorough review on concepts related to permeability definition (in saturated groundwater flow) is provided in [14]; see also the references therein. It was shown that the mesoscopic second-order symmetric permeability tensor $[\mathbf{K}]$ is a $\mathbb{M}_d^+(\mathbb{R})$-valued random variable, which means that it does exhibit *aleatoric* uncertainties, no matter the experimental protocol followed for characterization. Let us now consider the two following kinds of

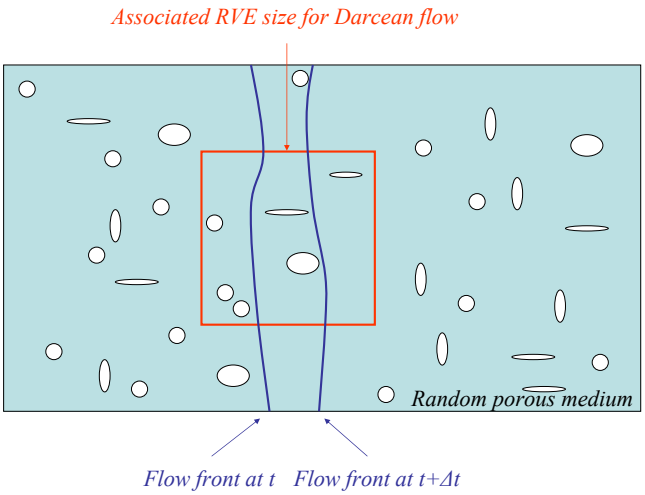

Figure 1: Schematic: definition of a mesoscale for the Darcean flow through a random porous medium.

boundary conditions:

(**i**) $p = \mathbf{p}_0 \cdot \mathbf{x}$ on $\partial\Omega$, $\mathbf{p}_0 \in \mathbb{R}^d$.

(**ii**) $\mathbf{v} \cdot \mathbf{n} = \mathbf{v}_0 \cdot \mathbf{n}$ on $\partial\Omega$, $\mathbf{v}_0 \in \mathbb{R}^d$ and $\mathbf{n}$ is the outward unit vector normal to the boundary $\partial\Omega$.

Boundary conditions (**i**) and (**ii**) are usually referred to as essential (or uniform) Dirichlet and natural (or uniform) Neumann boundary conditions, respectively. Equation (1) corresponds to the natural form of Darcy's law for Dirichlet boundary conditions and can be written as $\mathbf{v} = -(1/\mu)[\mathbf{K}^D]\boldsymbol{\nabla} p$, where the superscript D underlines the dependance on essential boundary conditions. Let us now rewrite Darcy's law as $\boldsymbol{\nabla} p = -\mu[\mathbf{R}^N]\mathbf{v}$, in which $[\mathbf{R}^N]$ is the matrix representation of a second-order symmetric positive-definite tensor (defined with respect to natural boundary conditions) that is referred to as the resistance tensor. It can then be shown that the apparent permeability and resistance tensors depend on the prescribed boundary conditions and are not inverse of one another (that is to say, $[\mathbf{K}^D][\mathbf{R}^N] \neq [I_d]$ almost surely -a.s.-) and $[\mathbf{R}^N]^{-1} \leq [\mathbf{K}^D]$ a.s. Further hierarchical properties for the permeability and resistance tensors can be found in [11] and can be seen as the counterpart, for permeability tensors, of Huet's partition theorem derived for elasticity tensors in [15] (see [16] for a review). Such properties imply that there is no unique permeability approximation at the mesoscale and underlines the key role played by the boundary conditions. The consequences of these properties on experimental analysis are note worthy (since they directly impact the identification of the model) but are beyond the scope of this study. From a theoretical standpoint, they further mean that at the mesoscale, the mapping relating the permeability tensor to local properties (describing the local pore space), such as porosity and tortuosity, is a stochastic function. Consequently, the idea, according to which the permeability tensor random field could be computed from such quantities as a byproduct (by having recourse, for instance, to the very widely used Kozeny-Carman equation [17] [18]), is not relevant to the retained framework of mesoscopic modeling for random media. Moreover, it should be stressed that proceeding this way would require the construction of probabilistic models for such morphological random fields, which is arguably intractable in practice due to the statistical dependence of such local properties.

From the discussion above, it follows that the apparent permeability has to be modeled as a non-Gaussian matrix-valued random field. The construction of an associated probabilistic model is precisely addressed below.

3 Stochastic modeling of permeability random fields

3.1 Choice of a stochastic framework and MaxEnt principle

In order to define the general framework of the approach, let $\mathbf{x}$ be fixed in the spatial domain under consideration and let $[\mathbf{K}(\mathbf{x})]$ be the $\mathbb{M}_d^+(\mathbb{R})$-valued random variable (with components $[\mathbf{K}(\mathbf{x})]_{ij}$), defined on a probability space $(\Theta, \mathcal{T}, \mathcal{P})$ and corresponding to the modeling of the stochastic permeability tensor.

Clearly, the random variable $[\mathbf{K}(\mathbf{x})]$ can be mapped onto a vectorial representation of its statistically dependent components, denoted by $\mathbf{K}(\mathbf{x})$. Since $\mathbf{K}(\mathbf{x})$ is a $\mathbb{R}^{d(d+1)/2}$-valued random variable, it follows that the probabilistic model has to be constructed, in general, on a space of high dimension. In particular, it is worth while to note that if the principal directions of the mean model are supposed to coincide with the axis of the general coordinate system, a simplifying assumption (which is usually followed for the sake of simplicity or because of a very limited experimental database) consists in modeling the random permeability as a diagonal matrix (or even as an almost sure isotropic tensor). However, such an assumption would imply, within a stochastic framework, that the principal permeabilities fluctuate, while the associated principal directions do not (and basically coincide with the principal directions of the mean model). As far as stochastic fluctuations are not negligible, such a fact is clearly inconsistent from a physical point of view, and especially if the framework of a mesoscale analysis is retained. Therefore, we may consider the case of a locally anisotropic and non-diagonal permeability tensor, under the additional constraint that some principal stochastic permeabilities may exhibit more statistical fluctuations than others. In soil mechanics, such tailored fluctuations could stem, in practice, from the existence of cracks with some preferred orientation for instance.

A tremendous amount of work has been published to address the issue of stochastic modeling for random permeability tensors. A large body of the literature provides results for UP, derived under particular conditions and assuming *a priori* probability distributions for the components of the permeability tensor (e.g. a log-normal distribution). Clearly, the conclusions drawn from such analysis are closely related to the retained assumptions and the issue of stochastic representation turns out to be as fundamental as the issue of UP. The use of functional representations has been proposed in [19] (see Section 3.2.4 and the references therein). However, such representations require, for calibration purposes, the permeability tensor to be measured at every point of the domain (and for a sufficiently large number of realisations of the random medium), which is seldom achievable in practice (note that a methodology to circumvent this difficulty has been proposed in [20] and can be readily applied to permeability tensor random fields). Since the randomness exhibited at a given scale stems from the underlying randomness occurring at finest scales, the definition of multi-scale representations for permeability tensors, based on Markov random fields, has been investigated in [21]. While theoretically appealing, such models still require the choice an a priori distribution for the mesoscopic permeability tensor and the calibration of the conditional distributions is certainly a tricky task. Since we are interested in constructing the most objective probabilistic model (i.e. without assuming *a priori* probability distributions) for the permeability tensor, we may proceed alternately. More specifically, the construction of the probabilistic model is achieved here following the methodology introduced in the definition of the so-called *non-parametric* framework, proposed in [22] [23] for analysing random uncertainties in dynamical systems. This approach is derived within the framework

of information theory, introduced by Shannon [24], and the stochastic model is derived having recourse to the Maximum Entropy (MaxEnt) principle [24] [25] [26] [27] [28] which is briefly recalled below.

For notational convenience, let us temporarily dropped out the spatial dependance on $\mathbf{x}$. Let $[K] \mapsto p_{[\mathbf{K}]}([K])$ be the probability density function, from $\mathbb{M}_d^+(\mathbb{R})$ into $\mathbb{R}^+$, defining the probability distribution $P_{[\mathbf{K}]} = p_{[\mathbf{K}]}([K])d[K]$ of random matrix $[\mathbf{K}]$. The measure $d[K]$ on $\mathbb{M}_d^S(\mathbb{R})$ is defined as:

$$d[K] = 2^{d(d-1)/4} \prod_{1 \leq i \leq j \leq d} d[K]_{ij}, \tag{2}$$

in which $d[K]_{ij}$ is the Lebesgue measure on $\mathbb{R}$. Let $\mathcal{C}_{ad}$ be the set of all the probability density functions from $\mathbb{M}_d^+(\mathbb{R})$ into $\mathbb{R}^+$ such that all the constraints defining the available information are fulfilled. The MaxEnt principle then states that:

$$p_{[\mathbf{K}]} = \underset{p \in \mathcal{C}_{ad}}{\arg\max}\ \mathrm{S}(p), \tag{3}$$

in which the measure of entropy $\mathrm{S}(p)$ of p is defined as:

$$\mathrm{S}(p) = -\int_{\mathbb{M}_d^+(\mathbb{R})} p([K]) \ln(p([K]))d[K], \tag{4}$$

wherein ln is the Neperian logarithm. In other words, the probability density function (p.d.f., in brief), estimated by using the MaxEnt principle, is the function which maximizes the measure of entropy (that is to say, the uncertainties) over the admissible space $\mathcal{C}_{ad}$. While such a procedure yields the most "objective" probabilistic model defined with respect to the available information, it must be emphasized that the definition of the admissible space $\mathcal{C}_{ad}$ (that is to say, of all the constraints fulfilled by the probability density function) is a key step, since unrelevant information may generate additional model uncertainties.

Two main sets of constraints can be basically distinguished. The first one is related to mathematical (algebraic) constraints which must be satisfied, such as the normalization of the p.d.f.:

$$\int_{\mathbb{M}_d^+(\mathbb{R})} p_{[\mathbf{K}]}\left([K]\right) \mathrm{d}[K] = 1. \tag{5}$$

Although this study is not devoted to uncertainty propagation, a fundamental issue which is worth while to note in this context of stochastic analysis concerns the resulting properties exhibited by the solution of the associated stochastic boundary value problem (see for instance [7] and [29] for discussions in the tensorial and scalar cases, respectively). In particular, it can be shown that the inverse of random matrix $[\mathbf{K}]$ is a second-order random variable if the following constraint holds [23]:

$$\int_{\mathbb{M}_d^+(\mathbb{R})} \ln\left(\det\left([K]\right)\right) p_{[\mathbf{K}]}\left([K]\right) \mathrm{d}[K] = \beta, \quad |\beta| < +\infty. \tag{6}$$

Equation (6), together with an additional constraint that will be introduced in Section 3.3 (see equation (28)), allows one to prove that the stochastic boundary value problem has a second-order stochastic solution [7]. Note that the positive-definiteness of the permeability tensor can be readily ensured by using a particular algebraic construction, as will be seen later on.

The second set of constraints is related to additional information that one would like to take into account. Since we are concerned with a probabilistic model constructed from a mean (or nominal) model,

it is desirable to specify the value $[\underline{K}]$ of the mean model as the mean value of random matrix $[\mathbf{K}]$, that is:

$$\mathrm{E}\left\{[\mathbf{K}]\right\} = \int_{\mathbb{M}_d^+(\mathbb{R})} [K]\, p_{[\mathbf{K}]}\left([K]\right) \mathrm{d}[K] = [\underline{K}]. \tag{7}$$

Finally, we may assume that the variances of the d stochastic eigenvalues of random matrix $[\mathbf{K}]$ are prescribed through the following constraint [30]:

$$\mathrm{E}\left\{\left(\underline{\boldsymbol{\varphi}}^{i\,\mathrm{T}}\,[\mathbf{K}]\,\underline{\boldsymbol{\varphi}}^{i}\right)^2\right\} = s_i^2\,\underline{\lambda}_i^2, \quad i \in [1,d], \tag{8}$$

wherein $\{(\underline{\lambda}_i, \underline{\boldsymbol{\varphi}}^i)\}_{i=1}^d$ is the set of eigenpairs (eigenvalues and orthonormal eigenvectors) of the mean matrix $[\underline{\mathrm{K}}]$. Introducing the Lagrange multipliers $\mu \in \mathbb{R}$, $(\alpha-1) \in \mathbb{R}$, $[\widetilde{M}] \in \mathbb{M}_d^S(\mathbb{R})$ and $\{\widetilde{\tau}_i \in \mathbb{R}^+\}_{i=1}^d$ associated with constraints (5-8), it can be easily deduced that the probability density function $[K] \mapsto p_{[\mathbf{K}]}([K])$, estimated by the MaxEnt principle, takes the form:

$$p_{[\mathbf{K}]}\left([K]\right) = k_1 \left(\det\left([K]\right)\right)^{\alpha-1} \exp\left(-\mathrm{tr}\left([\widetilde{M}]^{\mathrm{T}}[K]\right) - \sum_{i=1}^{d} \widetilde{\tau}_i \left(\underline{\boldsymbol{\varphi}}^{i\,\mathrm{T}}\,[K]\,\underline{\boldsymbol{\varphi}}^{i}\right)^2\right), \tag{9}$$

in which k_1 is a normalization constant. The Lagrange multipliers are therefore parameters of the probabilistic model (which can be identified by solving a stochastic inverse problem), the physical interpretation of which will be provided in Section 3.4.

In the next section, we make use of the above derivations in order to define a class of non-Gaussian positive-definite matrix-valued random fields, corresponding to the modeling of the permeability random field.

3.2 Probabilistic model for the permeability tensor random field

3.2.1 Algebraic definition

Let $\mathbf{x} \mapsto [\mathbf{K}(\mathbf{x})]$ be the $\mathbb{M}_d^+(\mathbb{R})$-valued permeability random field defined on probability space $(\Theta, \mathcal{T}, \mathcal{P})$, indexed by a bounded open domain $\mathcal{D}$ in $\mathbb{R}^{d^*}$.

Following 3.1, we assume that the mean function $\mathbf{x} \mapsto \mathrm{E}\{[\mathbf{K}(\mathbf{x})]\} = [\underline{K}(\mathbf{x})]$ of random field $\mathbf{x} \mapsto [\mathbf{K}(\mathbf{x})]$, defined from $\mathcal{D}$ into $\mathbb{M}_d^+(\mathbb{R})$, is known and that the following constraint holds for $1 \leq i \leq d$:

$$\mathrm{E}\left\{\left(\underline{\boldsymbol{\varphi}}^i(\mathbf{x})^{\mathrm{T}}\,[\mathbf{K}(\mathbf{x})]\,\underline{\boldsymbol{\varphi}}^i(\mathbf{x})\right)^2\right\} = s_i(\mathbf{x})^2\,\underline{\lambda}_i(\mathbf{x})^2, \tag{10}$$

in which $\{\underline{\lambda}_i(\mathbf{x})\}_{i=1}^d$ and $\{\underline{\boldsymbol{\varphi}}^i(\mathbf{x})\}_{i=1}^d$ are the sets of eigenvalues and orthonormal eigenvectors of $[\underline{K}(\mathbf{x})]$ (see also [31]). As stated earlier, the d deterministic functions $\mathbf{x} \mapsto s_i(\mathbf{x})$ are model parameters used for the formulation of the optimization problem in the MaxEnt procedure and allow, through equation (10) and the associated Lagrange multiplier field $\mathbf{x} \mapsto \widetilde{\tau}_i(\mathbf{x})$ (see Section 3.2.3), to constrain the variances of the d stochastic eigenvalues, that is to say, of the d stochastic principal permeabilities.

Following [30], let $[\underline{\Lambda}(\mathbf{x})]$, $[\underline{\Phi}(\mathbf{x})]$ and $[\underline{N}(\mathbf{x})]$ be the $(d \times d)$ matrices defined as:

$$[\underline{\Lambda}(\mathbf{x})] = \mathrm{diag}\left(\underline{\lambda}_1(\mathbf{x}), \ldots, \underline{\lambda}_d(\mathbf{x})\right), \tag{11}$$

$$[\underline{\Phi}(\mathbf{x})] = [\underline{\boldsymbol{\varphi}}^1(\mathbf{x}) \ldots \underline{\boldsymbol{\varphi}}^d(\mathbf{x})], \tag{12}$$

$$[\underline{N}(\mathbf{x})] = [\underline{K}(\mathbf{x})][\underline{\Phi}(\mathbf{x})][\underline{\Lambda}(\mathbf{x})]^{-1/2}. \tag{13}$$

It is readily seen that $[\underline{K}(\mathbf{x})] = [\underline{N}(\mathbf{x})][\underline{N}(\mathbf{x})]^{\mathrm{T}}$. For $\mathbf{x} \in \mathcal{D}$, we rewrite the random matrix $[\mathbf{K}(\mathbf{x})]$ as:

$$[\mathbf{K}(\mathbf{x})] = [\underline{N}(\mathbf{x})][\mathbf{H}(\mathbf{x})][\mathbf{H}(\mathbf{x})]^{\mathrm{T}}[\underline{N}(\mathbf{x})]^{\mathrm{T}}, \tag{14}$$

in which the random field $\mathbf{x} \mapsto [\mathbf{H}(\mathbf{x})]$, defined on probability space $(\Theta, \mathcal{T}, \mathcal{P})$ and indexed by $\mathcal{D}$, is defined having recourse to a nonlinear mapping (see Sections 3.2.3 and 3.2.4) of a set of $d(d+1)/2$ independent Gaussian random fields $\{\mathbf{x} \mapsto U_{i\ell}(\mathbf{x})\}_{1 \leq \ell \leq i \leq d}$, called the *stochastic germs* (see Section 3.2.2).

3.2.2 Definition of a set of stochastic germs

Let $\{\mathbf{x} \mapsto U_{i\ell}(\mathbf{x})\}_{1 \leq \ell \leq i \leq d}$ be a set of $d(d+1)/2$ independent second-order centered homogeneous Gaussian random fields, defined on probability space $(\Theta, \mathcal{T}, \mathcal{P})$, indexed by $\mathbb{R}^{d^*}$, with values in $\mathbb{R}$ and such that for all $\mathbf{x}$ in $\mathbb{R}^{d^*}$, $\mathrm{E}\{U_{i\ell}(\mathbf{x})^2\} = 1$.

Consequently, each germ $\mathbf{x} \mapsto U_{i\ell}(\mathbf{x})$ is defined, for $\mathbf{y} \in \mathbb{R}^{d^*}$, by an autocorrelation function $\mathbf{y} \mapsto \mathrm{R}_{U_{i\ell}}(\mathbf{y})$ which is written as:

$$\mathrm{R}_{U_{i\ell}}(\mathbf{y}) = \mathrm{E}\{U_{i\ell}(\mathbf{x}+\mathbf{y})U_{i\ell}(\mathbf{x})\} = \prod_{k=1}^{d^*} r_k^{i\ell}(y_k), \tag{15}$$

in which,

$$r_k^{i\ell}(0) = 1, \tag{16}$$

$$r_k^{i\ell}(y_k) = \left(\frac{2L_k^{i\ell}}{\pi y_k}\right)^2 \sin^2\left(\frac{\pi y_k}{2L_k^{i\ell}}\right) \text{ for } y_k \neq 0, \tag{17}$$

and $\{L_k^{i\ell}\}_{k=1}^{d^*}$ are the spatial correlation lengths of the germ $\mathbf{x} \mapsto U_{i\ell}(\mathbf{x})$.

3.2.3 Probability distributions

For $\mathbf{x}$ fixed in $\mathcal{D}$, $[\mathbf{H}(\mathbf{x})]$ is a lower triangular matrix-valued random variable, the components of which are denoted by $\{[\mathbf{H}(\mathbf{x})]_{i\ell}\}_{\ell=1}^{i}$. The random variables $\{[\mathbf{H}(\mathbf{x})]_{i\ell}\}_{\ell=1}^{i}$ are statistically dependent (but independent from the other elements $[\mathbf{H}(\mathbf{x})]_{k\ell}$, $k \neq i$). Let $\mathbf{H}(\mathbf{x})^{(i)}$ be the random vector $\mathbf{H}(\mathbf{x})^{(i)} = ([\mathbf{H}(\mathbf{x})]_{i1}, \ldots, [\mathbf{H}(\mathbf{x})]_{ii})$. Let $\mathbf{h}^{(i)}$ be the vector in $\mathbb{R}^i$ such that $\mathbf{h}^{(i)} = (\mathbf{h}_{i1}, \ldots, \mathbf{h}_{ii})$ and let $d\mathbf{h}^{(i)} = d\mathbf{h}_{i1} \times \ldots \times d\mathbf{h}_{ii}$ be the Lebesgue measure on $\mathbb{R}^i$.

For $\mathbf{x}$ *fixed* in $\mathcal{D}$, it can be deduced from equations (9) and (14) that the probability density function $\mathbf{h}^{(i)} \mapsto p_{\mathbf{H}(\mathbf{x})^{(i)}}(\mathbf{h}^{(i)}; \mathbf{x})$ on $\mathcal{C}_{(i)} = \mathbb{R}^{i-1} \times \mathbb{R}^+$, with respect to $d\mathbf{h}^{(i)}$, of random variable $\mathbf{H}(\mathbf{x})^{(i)}$ reads:

$$p_{\mathbf{H}(\mathbf{x})^{(i)}}(\mathbf{h}^{(i)}; \mathbf{x}) = c{\mathbf{h}_{ii}}^{d-1-i+2\alpha(\mathbf{x})} \exp\left(-\mu_i(\mathbf{x})(\sum_{\ell=1}^{i} {\mathbf{h}_{i\ell}}^2) - \tau_i(\mathbf{x})(\sum_{\ell=1}^{i} {\mathbf{h}_{i\ell}}^2)^2\right), \tag{18}$$

in which c is a normalization constant and $\tau_i(\mathbf{x}) = \widetilde{\tau}_i(\mathbf{x})\underline{\lambda}_i(\mathbf{x})^2$ for all $\mathbf{x}$ in $\mathcal{D}$. As mentioned above, the fields $\mathbf{x} \mapsto \alpha(\mathbf{x}) > 0$ and $\mathbf{x} \mapsto \tau_i(\mathbf{x}) \geq 0$ are parameters of the model, while the field $\mathbf{x} \mapsto \mu_i(\mathbf{x})$ can be expressed in terms of the two previous ones and is such that [32]:

$$\int_{\mathbb{R}^+} c_1 g^{(d+2\alpha(\mathbf{x})-1)/2} \exp\{-\mu_i(\mathbf{x})g - \tau_i(\mathbf{x})g^2\} dg = 1, \tag{19}$$

in which the normalization constant c_1 is given by:

$$c_1 = \left(\int_{\mathbb{R}^+} g^{(d+2\alpha(\mathbf{x})-3)/2} \exp\{-\mu_i(\mathbf{x})g - \tau_i(\mathbf{x})g^2\} dg \right)^{-1}. \tag{20}$$

By proceeding to the change of variable $r = \sqrt{2\tau_i(\mathbf{x})}g$ in equation (19), it is readily seen that:

$$\frac{\mathrm{U}_{\alpha(\mathbf{x})+n/2}\left(\mu_i(\mathbf{x})/\sqrt{2\tau_i(\mathbf{x})}\right)}{\mathrm{U}_{\alpha(\mathbf{x})+n/2-1}\left(\mu_i(\mathbf{x})/\sqrt{2\tau_i(\mathbf{x})}\right)} = \frac{\sqrt{2\tau_i(\mathbf{x})}}{\alpha(\mathbf{x})+(n-1)/2}, \tag{21}$$

in which $z \mapsto \mathrm{U}_a(z)$ is the parabolic cylinder function of parameter a and argument z. While solving equation (21) may be more attractive, from a computational standpoint, than solving equation (19), it is a very challenging task for some values of parameters $\alpha(\mathbf{x})$ and $\tau_i(\mathbf{x})$, regardless of the numerical approximation retained for U_a. In this case, one may alternatively proceed as follows. By combining equations (19) and (20), it is seen that $\mu_i(\mathbf{x})$ is such that:

$$\frac{\displaystyle\int_{\mathbb{R}^+} g^{(d+2\alpha(\mathbf{x})-1)/2} \exp\{-\mu_i(\mathbf{x})g - \tau_i(\mathbf{x})g^2\} dg}{\displaystyle\int_{\mathbb{R}^+} g^{(d+2\alpha(\mathbf{x})-3)/2} \exp\{-\mu_i(\mathbf{x})g - \tau_i(\mathbf{x})g^2\} dg} = 1. \tag{22}$$

By letting $\nu = -\mu_i(\mathbf{x})/(2\tau_i(\mathbf{x}))$, $\sigma^2 = 1/(2\tau_i(\mathbf{x}))$ and having recourse to the change of variable $g = \sigma x + \nu$, equation (22) reads, after some basic algebra:

$$\frac{\mathrm{E}\left\{\mathbb{I}_{[\mu_i(\mathbf{x})/\sqrt{2\tau_i(\mathbf{x})},+\infty[}(\mathcal{N})(\sigma\mathcal{N}+\nu)^{(d+2\alpha(\mathbf{x})-1)/2}\right\}}{\mathrm{E}\left\{\mathbb{I}_{[\mu_i(\mathbf{x})/\sqrt{2\tau_i(\mathbf{x})},+\infty[}(\mathcal{N})(\sigma\mathcal{N}+\nu)^{(d+2\alpha(\mathbf{x})-3)/2}\right\}} = 1, \tag{23}$$

in which $\mathbb{I}_{\mathcal{A}}(y) = 1$ if $y \in \mathcal{A}$ and $\mathbb{I}_{\mathcal{A}}(y) = 0$ otherwise, and where $\mathcal{N}$ is a normalized $\mathbb{R}$-valued Gaussian random variable. The l.h.s. of equation (23) can be estimated very efficiently, at a negligible computational cost, by using numerical Monte Carlo simulations (note however that the convergence of the estimate, with respect to the number of realisations, must be controlled). The resulting optimization problem turns out to be very stable, no matter the values of parameters $\alpha(\mathbf{x})$ and $\tau_i(\mathbf{x})$, and can be solved by using any suitable optimization algorithm.

3.2.4 Definition of the nonlinear mapping

Let $\mathbf{x}$ be fixed in $\mathcal{D} \subset \mathbb{R}^{d^*}$. Let $\mathbf{U}(\mathbf{x})^{(i)}$ be the random vector $\mathbf{U}(\mathbf{x})^{(i)} = (U_{i1}(\mathbf{x}), \ldots, U_{ii}(\mathbf{x}))$. Following Section 3.2.3, the nonlinear mapping between the random matrix $[\mathbf{H}(\mathbf{x})]$ and the germs $\{U_{i\ell}(\mathbf{x})\}$ can be defined row-wise as follows. Let $\chi^{(i)}$ be the function from $\mathbb{R}^i \times \mathcal{D}$ into $\mathcal{C}_{(i)}$, such that:

$$\mathbf{H}(\mathbf{x})^{(i)} = \chi^{(i)}(\mathbf{U}(\mathbf{x})^{(i)}, \mathbf{x}). \tag{24}$$

Since the probability density function of random vector $\mathbf{H}(\mathbf{x})^{(i)}$ is known explicitly (see equation (18)), several approaches, such as the use of the Rosenblatt transformation [33], are readily available for constructing such a mapping. However, such a transformation would require the numerical computation of

d multidimensional integrals, at all the points used in the discretization and for all realisations of the random field. Subsequently, a numerical approximation of this mapping can be defined as follows. For $2 \leq i \leq d$, let us first write random vector $\mathbf{H}(\mathbf{x})^{(i)}$ as (discrete Kahrunen-Loève decomposition [34]):

$$\mathbf{H}(\mathbf{x})^{(i)} = \underline{H}(\mathbf{x})^{(i)} + \sum_{j=1}^{i} \sqrt{\rho_j(\mathbf{x})}\eta_j(\mathbf{x})^{(i)}\psi^j(\mathbf{x}), \tag{25}$$

in which $\underline{H}(\mathbf{x})^{(i)} = \mathrm{E}\{\mathbf{H}(\mathbf{x})^{(i)}\}$, $\{\rho_j(\mathbf{x}), \psi^j(\mathbf{x})\}_{j=1}^{i}$ are the eigenvalues and eigenvectors of the covariance matrix of random vector $\mathbf{H}(\mathbf{x})^{(i)}$. The centered random vector $\boldsymbol{\eta}(\mathbf{x})^{(i)} = (\eta_1(\mathbf{x})^{(i)}, \ldots, \eta_i(\mathbf{x})^{(i)})$ is such that $E\{\boldsymbol{\eta}(\mathbf{x})^{(i)}\boldsymbol{\eta}(\mathbf{x})^{(i)^{\mathrm{T}}}\} = [I_i]$ and has an arbitrary probability distribution which is characterized by projecting $\boldsymbol{\eta}(\mathbf{x})^{(i)}$ onto the Gaussian polynomial chaos [35] [3] [36] and by taking random vector $\mathbf{U}(\mathbf{x})^{(i)}$ as the Gaussian germ of the expansion:

$$\boldsymbol{\eta}(\mathbf{x})^{(i)} \simeq \sum_{\gamma=1}^{N_{pce}} \mathbf{z}(\mathbf{x})^{(i)^{\gamma}}\Psi_\gamma(\mathbf{U}(\mathbf{x})^{(i)}), \tag{26}$$

in which $N_{pce} = (i + N_{ord})!/(i!N_{ord}!) - 1$ and N_{ord} is the truncation order of the expansion. The random variables $\{\Psi_\gamma(\mathbf{U}(\mathbf{x})^{(i)})\}_{\gamma=1}^{N_{pce}}$ are the normalized Hermite polynomials of the $\mathbb{R}^i$-valued Gaussian random variable $\mathbf{U}(\mathbf{x})^{(i)}$, renumbered for notational convenience. Finally, the set of deterministic $\mathbb{R}^i$-valued coefficients $\{\mathbf{z}(\mathbf{x})^{(i)^{\gamma}}\}_{\gamma=1}^{N_{pce}}$ is such that:

$$\sum_{\gamma=1}^{N_{pce}} \mathbf{z}(\mathbf{x})^{(i)^{\gamma}}\mathbf{z}(\mathbf{x})^{(i)^{\gamma\mathrm{T}}} = [I_i]. \tag{27}$$

The estimation of the fields of coefficients $\{\mathbf{x} \mapsto \mathbf{z}(\mathbf{x})^{(i)^{\gamma}}\}_{\gamma=1}^{N_{pce}}$ can be performed by combining a random search algorithm (sampling from the Stiefel manifold defined by equation (27)) with the Maximum Likelihood method (using realisations of $\mathbf{H}(\mathbf{x})^{(i)}$ synthesized from equation (18) by Markov Chain Monte Carlo or Slice sampling); see Section 4.2.

Assuming the mean-square convergence of the chaos expansion, the combination of equations (25) and (26) defines a numerical approximation of mapping $\chi^{(i)}$ that can be used for generating, from realisations of the Gaussian stochastic germs (see [37] for instance) and making use of equation (14), realisations of random field $\mathbf{x} \mapsto [\mathbf{K}(\mathbf{x})]$.

3.3 Fundamental properties

From the previous construction, one can easily deduce the following fundamental properties [31].

Property 3.1 $\forall \mathbf{x} \in \mathbb{R}^{d^*}$, $[\mathbf{K}(\mathbf{x})] \in \mathbb{M}_n^+(\mathbb{R})$ *almost surely.*

Property 3.2 $\forall \mathbf{x} \in \mathbb{R}^{d^*}$, $\mathrm{E}\{\|[\mathbf{K}(\mathbf{x})]\|_{\mathrm{F}}^2\} < +\infty$, *that is to say,* $\mathbf{x} \mapsto [\mathbf{K}(\mathbf{x})]$ *is a second-order random field.*

Property 3.3 *The mean function* $\mathbf{x} \mapsto \mathrm{E}\{[\mathbf{K}(\mathbf{x})]\}$ *is such that for all* $\mathbf{x}$ *in* $\mathbb{R}^{d^*}$, $\mathrm{E}\{[\mathbf{K}(\mathbf{x})]\} = [\underline{K}(\mathbf{x})]$.

Let $\mathbf{x} \mapsto [\mathbf{G}(\mathbf{x})]$ be the random field defined on probability space $(\Theta, \mathcal{T}, P)$, indexed by $\mathcal{D}$ and such that $[\mathbf{G}(\mathbf{x})] = [\mathbf{H}(\mathbf{x})][\mathbf{H}(\mathbf{x})]^{\mathrm{T}}$ and $E\{[\mathbf{G}(\mathbf{x})]\} = [I_n]$ for all $\mathbf{x}$ in $\mathbb{R}^{d^*}$. Let us assume that the following non-uniform ellipticity condition holds:

$$\mathrm{E}\left\{ \left(\sup_{\mathbf{x}\in\overline{\mathcal{D}}} \|[\mathbf{G}(\mathbf{x})]^{-1}\| \right)^2 \right\} = {c_{[\mathbf{G}]}}^2 < +\infty, \tag{28}$$

in which $\overline{\mathcal{D}}$ is the closure of $\mathcal{D}$, sup denotes the supremum, $\|\cdot\|$ is the operator norm and $c_{[\mathbf{G}]}$ is a positive finite constant. Note that the validity of equation (28), for given values of all the parameters, has to be controlled numerically. From equation (28), it can then be proven that [7]:

Property 3.4 *The associated stochastic boundary value problem has a unique, second-order solution* $\mathbf{x} \mapsto p(\mathbf{x})$.

From the construction above, it can be deduced that random field $\mathbf{x} \mapsto [\mathbf{K}(\mathbf{x})]$ is, in general, non-homogeneous. However, when all the parameterizing fields are independent of $\mathbf{x}$, random field $\mathbf{x} \mapsto [\mathbf{K}(\mathbf{x})]$ can be seen as the restriction to domain $\mathcal{D}$ of a homogeneous random field indexed by $\mathbb{R}^{d^*}$.

3.4 Physical interpretation of the parameterisation

From Sections 3.2.1 and 3.2.3, it can be deduced that the probabilistic model is completely parameterized by (**i**) the mean function $\mathbf{x} \mapsto [\underline{K}(\mathbf{x})] \in \mathbb{M}_n^+(\mathbb{R})$, (**ii**) the deterministic fields $\mathbf{x} \mapsto \alpha(\mathbf{x}) \in \mathbb{R}_*^+$ and $\mathbf{x} \mapsto \tau_i(\mathbf{x}) \in \mathbb{R}^+$, and (**iii**) the set of spatial correlation lengths $\{L_{i\ell}^k \in \mathbb{R}^+\}$, $1 \leq i \leq \ell \leq d$, $k = 1, \ldots, d^*$. For any random matrix $[\mathbf{A}]$, let $\delta_{[\mathbf{A}]}$ be the parameter allowing the level of statistical fluctuations of $[\mathbf{A}]$ to be characterized, defined as ${\delta_{[\mathbf{A}]}}^2 = \mathrm{E}\{\|[\mathbf{A}] - [\underline{A}]\|_{\mathrm{F}}^2\}/\|[\underline{A}]\|_{\mathrm{F}}^2$, where $[\underline{A}] = E\{[\mathbf{A}]\}$. For notational convenience and without loss of generality, let $\mathbf{x}$ be fixed in $\mathcal{D}$, so that spatial dependance is temporarily dropped out.

From [30], it can be deduced that:

$${\delta_{[\mathbf{G}]}}^2 = \frac{1}{n}\sum_{j=1}^{n} s_i^2 - \frac{2\alpha}{2\alpha + n - 1}. \tag{29}$$

From equations (10) and (29), it is readily seen that $\alpha \to +\infty$ implies that $\delta_{[\mathbf{G}]} \to 0$ and therefore, making use of equation (14), that $[\mathbf{K}] \to [\underline{K}]$ in probability. Equation (29) further implies that for given values of s_i ($1 \leq i \leq d$), belonging to some admissible spaces (which cannot be explicitly described), the value of parameter α must be selected in order to generate a given overall level of statistical fluctuations (in view of an inverse identification based on experimental results, for instance) for the random permeability $[\mathbf{K}]$.

Moreover, for a given value of α, numerical investigations show that the field $\mathbf{x} \mapsto \tau_i(\mathbf{x})$ has a negligible effect on the mean value $\mathrm{E}\{\lambda_i\}$ of the stochastic eigenvalue λ_i, but allows for a significant reduction of its variance when $\tau_i \to +\infty$ (see [32], as well as Section 4). Consequently, parameter τ_i must be selected (or identified) in order to ensure a given level of statistical fluctuation for the associated stochastic principal permeability λ_i.

It is worth noticing that the probabilistic model proposed in [7] could be used for modeling a stochastic permeability field as well. Nevertheless, it is interesting to note that this other non-parametric model can be recovered by setting all parameters τ_i to a null value and basically induces the same level of statistical fluctuations on all the components of the random matrix $[\mathbf{K}]$. Such a property implies, therefore, that all

the principal stochastic permeabilities would exhibit the same level of fluctuations, no matter the local morphology of the porous medium. On the contrary, we will show in Section 4 that the probabilistic model proposed in this work allows specifying different levels of uncertainties in given directions and within a non-parametric framework, making it a very powerful tool for Darcean flow simulations and identification.

3.5 Summary and general algorithmic scheme

We summarize below the general algorithm allowing independent realizations of random field $\mathbf{x} \mapsto [\mathbf{K}(\mathbf{x})]$ to be generated. Note that for the sake of readability, the parameter fields are assumed to be constant over domain $\mathcal{D}$ in the sequel (the generalization of the scheme to non-constant fields being straightforward).

- **Step 1: preprocessing**

  (**i**) Select appropriate values for parameters $[\underline{K}]$ (mean value), α (controlling the overall level of statistical fluctuations of $[\mathbf{K}(\mathbf{x})]$) and τ_i (controlling the variance of the associated random eigenvalue λ_i), $i = \{1, \ldots, d\}$.

  (**ii**) Compute matrix $[\underline{N}]$ defined by Eq. (13).

  (**iii**) Compute parameters μ_i, $i = \{1, \ldots, d\}$, solving Eq. (23).

  (**iv**) For $i = \{2, \ldots, d\}$, compute the numerical approximation of nonlinear mapping $\chi^{(i)}$ (defined in Section 3.2.4) as follows:

  - Generate independent realizations of random vector $\mathbf{H}^{(i)}$ using Eq. (18).
  - Perform the statistical reduction using Eq. (25) and compute the independent realizations of random vector $\boldsymbol{\eta}^{(i)}$.
  - Compute the coefficients involved in the chaos expansion (26).

- **Step 2: main loop for numerical monte carlo simulations**

  (**i**) For $1 \leq \ell \leq i \leq d$, compute an independent realization of random fields $\mathbf{x} \mapsto U_{i\ell}(\mathbf{x})$.

  (**ii**) For each point $\mathbf{x}$ in $\mathcal{D}$, compute the realization of random matrix $[\mathbf{H}(\mathbf{x})]$ associated with the realization of the germs (generated in Step 2 (**i**)) using the approximations of mappings $\chi^{(i)}$, $i = \{1, \ldots, d\}$, computed in Step 1 (**iv**).

  (**iii**) For each point $\mathbf{x}$ in $\mathcal{D}$, compute the realization of random matrix $[\mathbf{K}(\mathbf{x})]$ by using (14).

4 Parametric study and illustration

The aim of this final section is twofold. Firstly, we exemplify, in Section 4.1, the role of each parameter $\alpha(\mathbf{x})$ and $\tau_i(\mathbf{x})$. In particular, we demonstrate the capability of the model to deal with non-homogeneous constraints on the principal stochastic permeabilities. Secondly, we illustrate the overall methodology (and more specifically, the procedure for identifying the chaos coefficients) for generating realisations of the permeability random field $\mathbf{x} \mapsto [\mathbf{K}(\mathbf{x})]$ in Section 4.2.

4.1 Parametric study on parameters

For illustration purposes, let us first consider the two dimensional case and fix $\mathbf{x}$ in $\mathcal{D}$, so that the probabilistic results can be easily interpreted from a physical point of view. Let λ_x and λ_y be the two stochastic principal permeabilities of random tensor $[\mathbf{K}]$. We denote by $\ell \mapsto p_{\lambda_x}(\ell)$ (resp. $\ell \mapsto p_{\lambda_y}(\ell)$) the probability density function of λ_x (resp. λ_y). Accordingly, we denote by τ_x (resp. τ_y) the parameter associated with λ_x (resp. λ_y). Let θ be the random variable corresponding to the modeling of the rotation angle defining the transformation between the reference coordinate frame and the frame defined by the stochastic principal directions. Let $w \mapsto p_\theta(w)$ be the probability density function of θ. Without loss of generality, we may assume that the axis of the reference frame coincide with the principal directions of the mean model. Finally, let the mean model be very slightly anisotropic and defined by (in 10^{-10} m^2):

$$[\underline{K}] = \begin{bmatrix} 1.05 & 0 \\ 0 & 0.95 \end{bmatrix}. \tag{30}$$

4.1.1 Influence of parameters α, τ_x and τ_y

First of all, let the variances of random variables λ_x and λ_y be constrained in a similar way and let $\tau_x = \tau_y = 10^2$. For $\alpha = 20$ (resp. $\alpha = 50$ and $\alpha = 80$), the overall level of statistical fluctuations of random matrix $[\mathbf{K}]$ can be estimated from usual mathematical statistics and is found to be $\delta_{[\mathbf{K}]} = 0.17$ (resp. $\delta_{[\mathbf{K}]} = 0.12$ and $\delta_{[\mathbf{K}]} = 0.10$). In agreement with 3.4, it is seen that the parameter α mainly controls the fluctuations of $[\mathbf{K}]$. This conclusion can also be drawn from Figure 2, in which the probability density functions of the stochastic principal permeabilities (in 10^{-10} m^2) are plotted for $\tau_x = \tau_y = 10^2$ and $\alpha = 20$ (dash-dot line), $\alpha = 50$ (solid line) and $\alpha = 80$ (dashed line). The probability density

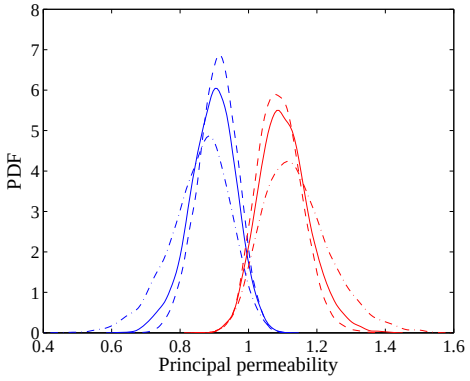

Figure 2: Plot of the probability density function of λ_x (red line) and λ_y (blue line), in 10^{-10} m^2, for $\tau_x = \tau_y = 10^2$ and $\alpha = 20$ (dash-dot line), $\alpha = 50$ (solid line) and $\alpha = 80$ (dashed line).

functions of the stochastic principal permeabilities λ_x and λ_y are plotted in Figure 3, for $\alpha = 60$ and $\tau_x = \tau_y = \tau \in \{1, 10, 10^2, 10^3, 10^4\}$. It is readily seen that imposing large values of parameter τ allows one to significantly reduce the variance of the stochastic principal permeabilities. It is worth pointing out that since the eigenvalues of $[\mathbf{K}]$ remain stochastic, their variances can be prescribed over a given, limited range of values.

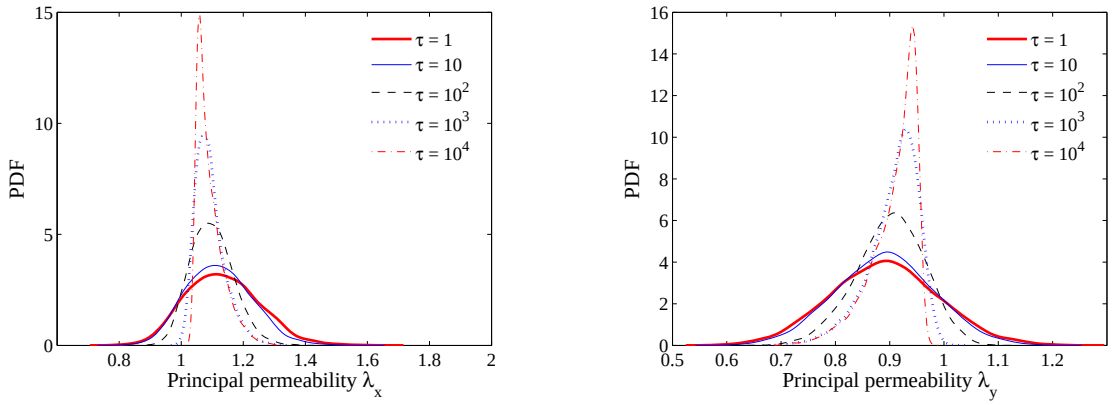

Figure 3: Plot of the probability density functions of λ_x (left) and λ_y (right), for $\alpha = 60$ and different values of $\tau_x = \tau_y = \tau$.

4.1.2 On generating different levels of fluctuations in given directions

In the previous section, we exemplified the role played by parameters α and τ, for similar variance constraints (that is to say, for $\tau_x = \tau_y$). Here, we investigate non homogeneous constraints and consider the two following cases $\{\alpha = 80, \tau_x = 10^4, \tau_y = 1\}$ and $\{\alpha = 80, \tau_x = 1, \tau_y = 10^4\}$. The convergence of the norm $\left\{\mathrm{E}\{\|[\mathbf{K}]\|_{\mathrm{F}}^2\}\right\}^{1/2}$ with respect to the number of Monte-Carlo simulations is first characterized in Figure 4. It is seen that a reasonable level of convergence is achieved for 3 000 simulations. In both

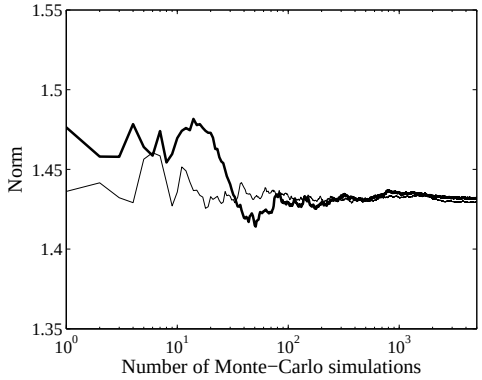

Figure 4: Plot of the convergence of $\left\{\mathrm{E}\{\|[\mathbf{K}]\|_{\mathrm{F}}^2\}\right\}^{1/2}$ with respect to the number of Monte-Carlo simulations. Thin solid line: $\alpha = 80$, $\tau_x = 10^4$ and $\tau_y = 1$. Thick solid line: $\alpha = 80$, $\tau_x = 1$ and $\tau_y = 10^4$.

cases, the level of statistical fluctuations of random matrix $[\mathbf{K}]$ is found to be $\delta_{[\mathbf{K}]} = 0.12$. The probability density functions of λ_x (red dashed line) and λ_y (blue solid line), estimated from 5 000 independent realisations using the kernel density estimation method [38], are plotted in Figure 5 for the first and

second set of parameters, respectively. As expected, setting a large value of parameter τ allows for a

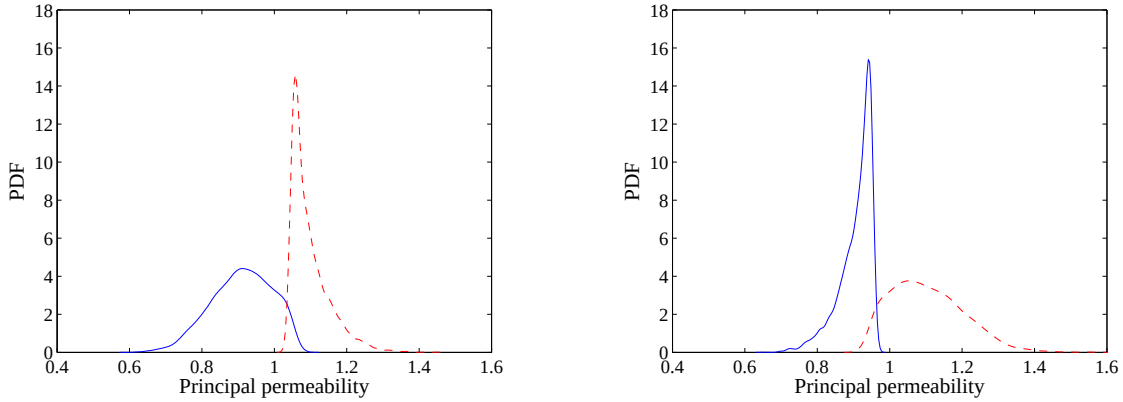

Figure 5: Plot of the probability density function of the first (red dashed line) and second (blue solid line) stochastic principal permeability (in 10^{-10} m^2). Left: $\alpha = 80$, $\tau_x = 10^4$ and $\tau_y = 1$. Right: $\alpha = 80$, $\tau_x = 1$ and $\tau_y = 10^4$.

significant reduction of the variance of the associated stochastic principal permeability. Comparing theses two Figures, it is readily seen that while the random permeability tensor exhibits exactly the same overall level of statistical fluctuations, a larger level of fluctuations can be imposed in a given, chosen direction. For the first set of parameters ($\alpha = 80$, $\tau_x = 10^4$ and $\tau_y = 1$), the mean and coefficient of variation of the stochastic principal permeability λ_x (resp. λ_y) are 1.1 and 4.9% (resp. 0.9 and 9%). For the second case ($\alpha = 80$, $\tau_x = 1$ and $\tau_y = 10^4$), the mean and coefficient of variation of λ_x (resp. λ_y) are 1.1 and 4.9% (resp. 0.9 and 9%). Finally, the probability density function $w \mapsto p_\theta(w)$ of the rotation angle (in degrees) is shown in Figure 6.

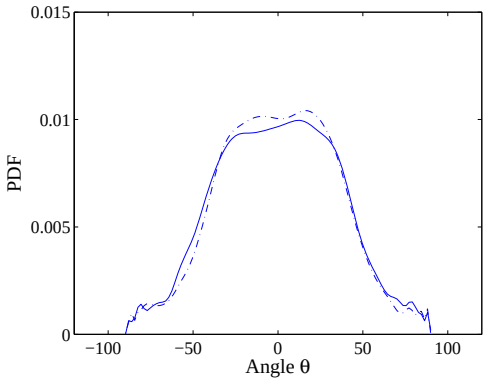

Figure 6: Plot of the probability density function of random variable θ. Blue solid line: $\alpha = 80$, $\tau_x = 10^4$, $\tau_y = 1$. Dashed solid line: $\alpha = 80$, $\tau_x = 1$, $\tau_y = 10^4$.

For the type of (symmetric) constraints considered, it is seen that parameter τ has a negligible influence on the angle of rotation θ. This fact can be easily explained by the orthogonality of the principal directions and means that while different levels of uncertainties can be assigned to given components, the related stochastic principal directions cannot be specifically constrained.

4.2 Illustration for random field applications

For all $\mathbf{x}$ in $\mathcal{D} =]0, 20[^2$, let us consider the following set of parameters: $\alpha(\mathbf{x}) = 60$, $\tau_1(\mathbf{x}) = \tau_2(\mathbf{x}) = 500$, $[\underline{K}(\mathbf{x})] = [\underline{K}]$ (in which $[\underline{K}]$ is given by equation (30)). The spatial correlation lengths (for all the stochastic germs) are assumed to be all equal to $L = 4$. Hence, mappings $\chi^{(1)}$ and $\chi^{(2)}$ do not depend on $\mathbf{x}$ anymore, and random matrix $[\mathbf{H}]$ takes the form:

$$[\mathbf{H}] = \begin{pmatrix} h_{11} & 0 \\ h_{21} & h_{22} \end{pmatrix}. \tag{31}$$

In order to facilitate the identification of the chaos expansion for the random variable h_{11} and following Section 3.2.4, let us first write h_{11} as:

$$h_{11} = \sigma_{h_{11}} \rho^{(1)} + \underline{h}_{11}, \tag{32}$$

wherein $\underline{h}_{11}$ and $\sigma_{h_{11}}$ are the mean and standard deviation of h_{11} and $\rho^{(1)}$ is a centred random variable with unit variance. Introducing the chaos expansion of $\rho^{(1)}$, $\rho^{(1)} = \sum_{k=1}^{N_{pce}-1} z_k^{(1)} \Psi_k(\xi)$ (in which ξ is a normalized Gaussian random variable and Ψ_k is the one-dimensional Hermite polynomial of order k), it can be deduced that the real-valued coefficients $\{z_k^{(1)}\}_{k=1}^{N_{pce}-1}$ are such that $\sum_{k=1}^{N_{pce}-1} {z_k^{(1)}}^2 = 1$. Therefore, the identification of the chaos coefficients can be performed by taking advantage of the well-known parameterisation of the unit hypersphere in $\mathbb{R}^{N_{pce}-1}$, using a random search algorithm and the Maximum Likelihood principle. Here, the identification has been performed by using 1 000 realisations of $\rho^{(1)}$ (computed by using equation (32)) and a $10th-$order chaos expansion. Figure 7 displays the reference p.d.f. of $\rho^{(1)}$ (thin solid line), as well as the p.d.f. estimated from realisations generated by using the chaos expansion with the optimal set of coefficients (thick solid line). It is seen that the two functions compare well, even for small levels of probability.

Following Section 3.2.4, a numerical approximation of mapping $\chi^{(2)}$ is constructed by using equations (25) and (26). The deterministic coefficients involved in the $4th-$ order chaos expansion of the random vector $\boldsymbol{\eta}^{(2)} = ({\eta_1}^{(2)}, {\eta_2}^{(2)})$ is performed by having recourse to the Maximum Likelihood method on first-order marginal distributions (see [39] for a discussion) and using a slightly modified version of the algorithm proposed in [20]. For this purpose, we considered 1 000 realisations of $\boldsymbol{\eta}^{(2)}$, computed from the realisations of $\mathbf{H}^{(2)} = (h_{21}, h_{22})$ by using the orthonormality of the eigenvectors in equation (25). Figure 8 displays the graphs of the target (thin line) and simulated (thick line) p.d.f. of random variables ${\eta_1}^{(2)}$ (left) and ${\eta_2}^{(2)}$ (right) and shows the good convergence of the chaos expansion. It should be mentioned that the orders of the chaos expansion have been determined from a convergence analysis. Once the numerical approximations of the non-linear mappings have been constructed (as a preliminary step), realisations of random field $\mathbf{x} \mapsto [\mathbf{K}(\mathbf{x})]$ can be readily obtained from Monte-Carlo simulations of the Gaussian stochastic germ and by using equations (26), (25) and (14). A realisation of the stochastic permeability random fields, defined by the parameters given above, is displayed on Figure 9.

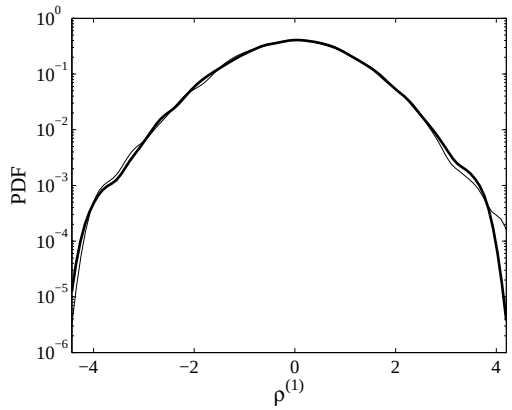

Figure 7: Plot (in semi-log scale) of the p.d.f. of random variable $\rho^{(1)}$: target (thin solid line) and chaos expansion estimate (thick solid line).

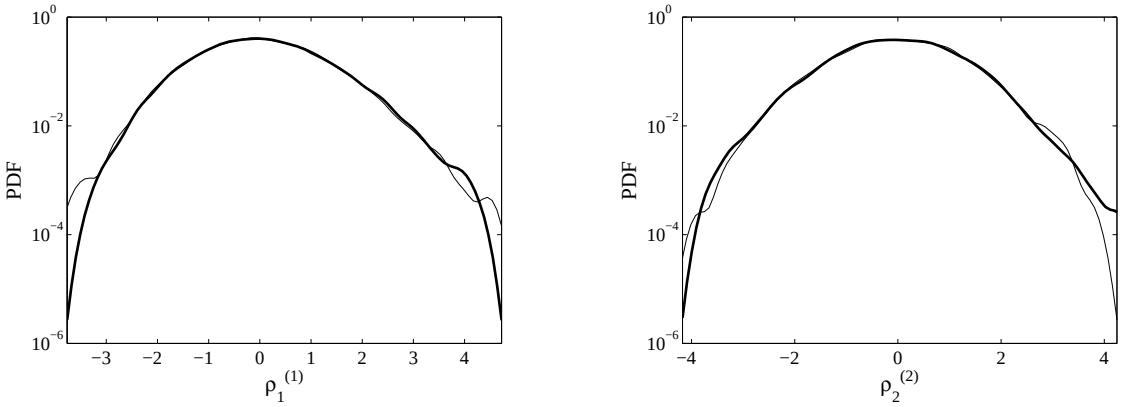

Figure 8: Plot (in semi-log scale) of the probability density function $p_{\eta_j{}^{(2)}}$. Reference: thin solid line; Estimation based on chaos expansion: thick solid line. Left: $j = 1$; Right: $j = 2$.

5 Conclusion

In this paper, we have presented a novel stochastic model for non-Gaussian anisotropic permeability tensor random fields. Such an issue is critical for accurately simulating Darcean flows through random porous media that do not exhibit a scale separation.

We first discussed the nature of the uncertainties exhibited by the apparent permeability tensors. Beyond the epistemic uncertainties generated by the experimental characterization procedure, results reported in the literature show that the permeability tensor is intrinsically random if the scale separation is not achieved.

Subsequently, we proposed a probabilistic model for modeling such permeability tensor random fields,

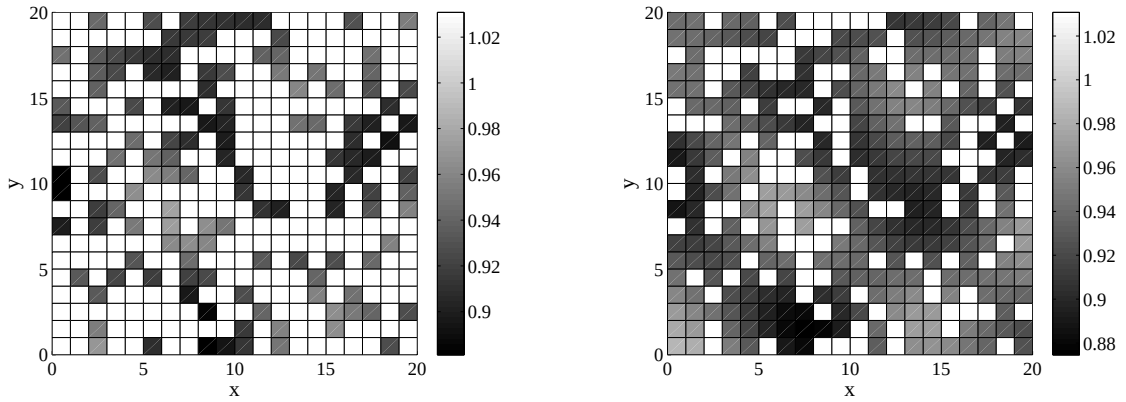

Figure 9: Plot of a realisation of random fields $\mathbf{x} \mapsto \lambda_x(\mathbf{x})$ (left) and $\mathbf{x} \mapsto \lambda_y(\mathbf{x})$ (right).

the construction of which is performed within the framework of information theory. The stochastic representation therefore differs from all other probabilistic models for permeability tensors available in the literature and does not introduce any modeling bias which could stem from the choice of a probability distribution *a priori*. We have investigated the capability of the above class of random fields to deal with non-homogeneous constraints. Unlike the few other non-parametric models that were previously derived and applied for modeling other physical tensor-valued random fields (such as the elasticity tensor random field), it was shown that the considered class of random fields allows assigning higher levels of statistical fluctuations for given stochastic principal permeabilities, while keeping the overall fluctuations of the random permeability tensor constant. It should be pointed out that such a property is intrinsic to the modeling of the permeability tensor (since the constraints directly act on the quantities of interest, that are, the random principal permeabilities) and would not generally hold, should the stochastic representation be applied to another physical property (elasticity tensor, etc.).

Thus, the flexibility offered by the parametrization opens up many new possibilities in terms of stochastic simulations involving random permeability tensors. The choice of the parameterisation may be guided by either the local microstructure of the medium (assigning higher fluctuations for some components) or difficulties to measure the permeability in a specific direction. The probabilistic model further allows the use of non-homogeneous fields $\mathbf{x} \mapsto \tau_i(\mathbf{x})$, which could be chosen such that homogeneous uncertainties (that is to say, imposing the same level of uncertainties on all the stochastic principal permeabilities) are generated on some given parts of the domain, while specific constraints (i.e. higher statistical fluctuations in some directions) are considered on some other parts. This feature could be used, for instance, for modeling the presence of cracks in the study of Darcean flows through damaged media.

By taking care of the local anisotropy of the random permeability tensor, the proposed model is capable of generating physically-sounded realisations and may pave the way for predictive stochastic simulations of Darcean flows in high probabilistic dimensions.

References

[1] Yeh WWG. Review of parameter identification procedures in groundwater hydrology: The inverse problem. *Water Ressources Research* 1986; **22**:95–108.

[2] Rubin Y. *Applied Stochastic Hydrogeology*. Oxford Univ. Press, 2003.

[3] Ghanem RG, Spanos PD. *Stochastic Finite Elements: A Spectral Approach (rev. ed.)*. Dover Publications, 2003.

[4] Le Maître OP, Knio OM. *Spectral Methods for Uncertainty Quantification: With Applications to Computational Fluid Dynamics*. Springer, 2010.

[5] Zhang D. *Stochastic Methods for Flow in Porous Media: Coping with Uncertainties*. Academic Press, 2001.

[6] Schuëller GIE. A state-of-the-art report on computational stochastic mechanics. *Probabilistic Engineering Mechanics* 1997; **12**:197–321.

[7] Soize C. Non-gaussian positive-definite matrix-valued random fields for elliptic stochastic partial differential operators. *Computer Methods in Applied Mechanics and Engineering* 2006; **195**:26–64.

[8] Martys N, Garboczi EJ. Length scales relating the fluid permeability and electrical conductivity in random two-dimensional model porous media. *Physical Review B* 1992; **46**:6080–6090.

[9] Torquato S. *Random Heterogeneous Materials: Microstructure and Macroscopic Properties*. Springer, 2001.

[10] Rubinstein J, Torquato S. Flow in random porous media: mathematical formulation, variational principles, and rigorous bounds. *Journal of fluid mechanics* 1989; **206**:25–46.

[11] Du X, Ostoja-Starzewski M. On the size of representative volume element for darcy law in random media. *Proc. R. Soc. A* 2006; **462**:2949–2963.

[12] Pouya A, Courtois A. Permeability of 3d discontinuity networks: New tensors from boundary-conditioned homogenisation. *Advances in Water Resources* 2009; **32**:303–314.

[13] Yue X, Weinan E. The local microscale problem in the multiscale modeling of strongly heterogeneous media: Effects of boundary conditions and cell size. *Journal of Computational Physics* 2007; **222**:556–572.

[14] Sanchez-Vila X, Guadagnini A, Carrera J. Representative hydraulic conductivities in saturated groundwater flow. *Rev. Geophys.* 2006; **44**:25–46.

[15] Huet C. Application of variational concepts to size effects in elastic heterogeneous bodies. *Journal of the Mechanics and Physics of Materials* 1990; **38**:813–841.

[16] Ostoja-Starzewski M. *Microstructural Randomness and Scaling in Mechanics of Materials*. Chapman and Hall-CRC, 2008.

[17] Kozeny J. Über capillare leitung des wassers im boden. *Sitzungsber, Akad. Wiss. Wien* 1927; **136**:271–306.

[18] Carman PC. Fluid flow through granular beds. *Transactions of the Institution of Chemical Engineers* 1937; **15**:150–166.

[19] Ghanem RG. Probabilistic characterization of transport in heterogeneous media. *Computer Methods in Applied Mechanics and Engineering* 1998; **158**:199–220.

[20] Soize C. Identification of high-dimension polynomial chaos expansions with random coefficients for non-gaussian tensor-valued random fields using partial and limited experimental data. *Computer Methods in Applied Mechanics and Engineering* 2010; **199**:2150–2164.

[21] Ferreira MAR, Lee HKH. *Multiscale Modeling: A Bayesian Perspective*. Springer, 2007.

[22] Soize C. A nonparametric model of random uncertainties on reduced matrix model in structural dynamics. *Probabilistic Engineering Mechanics* 2000; **15**:277–294.

[23] Soize C. Maximum entropy approach for modeling random uncertainties in transient elastodynamics. *Journal of the Acoutical Society of America* 2001; **109**:1979–1996.

[24] Shannon CE. A mathematical theory of communication. *Bell System Technical Journal* 1948; **27**:379–423/623–659.

[25] Jaynes ET. Information theory and statistical mechanics. *Physical Review* 1957; **106**:620–630.

[26] Jaynes ET. Information theory and statistical mechanics. *Physical Review* 1957; **108**:171–190.

[27] Kapur JN, Kesavan HK. *Entropy Optimization Principles with Applications*. Academic Press, 1992.

[28] Cover TM, Thomas JA. *Elements of Information Theory*. John Wiley & Sons, 2006.

[29] Babuška I, Nobile F, Tempone R. A stochastic collocation method for elliptic partial differential equations with random input data. *SIAM Rev.* 2010; **52**:317–355.

[30] Mignolet MP, Soize C. Nonparametric stochastic modeling of linear systems with prescribed variance of several natural frequencies. *Probabilistic Engineering Mechanics* 2008; **23**:267–278.

[31] Guilleminot J, Soize C. Non-gaussian positive-definite matrix-valued random fields with constrained eigenvalues: application to random elasticity tensors with uncertain material symmetries. *Submitted for publication* 2010; .

[32] Guilleminot J, Soize C. A stochastic model for elasticity tensors with uncertain material symmetries. *International Journal of Solids and Structures* 2010; **47**:31213130.

[33] Rosenblatt M. Remark on a multivariate transformation. *The Annals of Mathematical Statistics* 1952; **23**:470–472.

[34] Loève M. *Probability Theory II (4th edn)*. Springer, 1978.

[35] Wiener N. The homogeneous chaos. *American Journal of Mathematics* 1938; **60**:897–936.

[36] Soize C, Ghanem RG. Physical systems with random uncertainties: chaos representations with arbitrary probability measure. *SIAM Journal on Scientific Computing* 2004; **26**:395–410.

[37] Shinozuka M. Simulations of multivariate and multidimensional random processes. *Journal of Acoustical Society of America* 1971; **39**:357–367.

[38] Bowman AW, Azzalini A. *Applied Smoothing Techniques for Data Analysis*. Oxford University Press, 1997.

[39] Desceliers C, Ghanem R, Soize C. Maximum likelihood estimation of stochastic chaos representations from experimental data. *International Journal for Numerical Methods in Engineering* 2006; **66**:978–1001.